# Investigation of dissimilar Joints between AA7075-T6 and AZ31B-H24 with and without interlayers produced by friction stir welding

Mahmoud Abbas1, Mohamed Zaki 2, Hamed Abdelaleem 3, Bassam Ghareeb 4

Suez University, Faculty of Petroleum and Mining Engineering, Metallurgical and Material Engineering, Dep. Assalam City, Suez, P.O. Box 43533, Egypt.

1Email: prof_abbas@hotmail.com, 2Email:Bassam@eliteservices-int.com

Metallurgical and Material Engineering

## Abstract

Multi-material lightweight structures are gaining a great deal of attention in several industries, especially the aerospace and automobile industry, great emphasis has been placed upon aluminium and magnesium alloys due to their high specific strength, improved performance and low density among other unique properties. Welding of dissimilar Mg and Al is challenging due to the formation of brittle intermetallic compound (IMCs) such as Mg17Al12 and Mg2Al3. In order to increase the joint strength and obtain defect free joining of light alloys , two main approaches were used to eliminate or reduce the Mg-Al intermetallic reaction layer. First, Control important processing parameters of solid state welding technique, FSW which have a low welding temperature were used to reduce the IMCs. Second, Employing interlayers such as Ni and Zn foil during welding of Al to Mg could be a feasible approach to eliminate intermetallic and improve mechanical and electrochemical properties of the joints. Effect of different interlayers and some important processing parameters and their effects on weld quality are discussed, and the microstructure and metallurgical reaction are described. Mechanical properties of welds such as hardness and tensile are discussed.


**Keywords:** aluminium alloys; magnesium alloys; Friction stir welding; Ni interlayer; Zn interlayer; intermetallic compound; mechanical property.

## 1. Introduction

Aluminum alloys have been extensively applied in different industries such as electronics, aerospace, shipbuilding and automotive, given their outstanding characteristics, namely good formability, high strength, good corrosion resistance and low weight. Magnesium alloys have always been attractive to designers due to their low density, only two thirds that of aluminium alloys in the aerospace industry and therefore can be an innovation technology if used for low weight structures. In fact, various Al and Mg alloys are anticipated to become the fundamental materials in almost all structures in the near future. Therefore significant frontloading is made to develop Al/Mg hybrid structures to achieve further light-weighting. Unfortunately, the conventional fusion welding techniques are proven unattractive to join Al to Mg alloys due to high potential to have some defects such as liquation induced cracking and porosity because of entrapped hydrogen inside of the weld bead, during solidification massive intermetallic compounds (IMCs) formation in the weld zone, which is a key factor to deteriorate the joint quality, thus limiting their industrial applications.

Due to its solid-state nature, friction stir welding (FSW) is a promising approach to join dissimilar Al and Mg alloys. The localized nucleation of brittle IMCs can be controlled due to reduced heat input, thus improving the joint strength. In dissimilar alloys welding, the IMCs formation is critical and pay special attention to produce high-quality weld joints. Previous studies have pointed out that a complete elimination of IMCs is hardly obtainable. However, their magnitude can be diminished. The weld local regions with massive IMCs accumulation enhance the crack propagation and fail via brittle fracture.

The diffusion of Al and Mg can also be minimized by adding a metallic interlayer between the metals. This interlayer may work as a barrier to limit the movement and mixing of

Al and Mg atoms. Consequently, Al-Mg IMCs can be eliminated or significantly reduced, and joints with better strength can be obtained.

At low temperatures, Zn preferably reacts with Mg to yield Mg-Zn IMCs, based on the phase diagrams of Mg-Zn and Al-Zn. Furthermore, a large solid solubility may be formed between Zn and Al, which causes Zn to function as an alloying element and improves the mechanical characteristics of the FSW Mg-Al joint, the significant part of Zn interlayer in joining Al and Mg alloys is obvious since Zn can prevent the excessive reaction between Al and Mg atoms. This phenomenon inhibits Mg-Al IMC formation. improving therefore the mechanical properties of the joints.

The Ni interlayer can be selected due to its substantial solid solubility with Al and Mg alloys than other materials, . The Gibbs free energies for the Al-Mg, Al-Ni, and Mg-Ni IMCs and phase diagrams indicate that Ni interlayer can work as an effective reaction barrier during Al-Mg dissimilar joining. Besides, the lowest eutectic temperatures encountered for the Al-Ni and Mg-Ni systems (916 °C and 506 °C, respectively) are significantly higher than that with the Al-Mg system (437 °C). It also emphasizes that Ni interlayer can be efficacious to minimize the solidification cracks during the fusion welding process, however in FSW no fusion is encompassed, the melting of the Ni interlayer is not anticipated as the melting point temperature of Ni (1453 °C) is significantly higher than the average maximum temperature reported in the FSW process (450-550 °C). During the FSLW, the sheared interlayer is transformed into the broken tiny flakes in the weld zone. Some of these get intermixed with the Al and Mg substrates, while the rest remain stick at various places with the hook region. As the Ni strips are found to be stick with the Al and Mg substrates, it signifies that some wetting reaction might have occurred between the Mg-Ni and Al-Ni.

## 2 Experiments

### 2.1 Materials

In this study, Three Samples of AA7075-T6 and AZ31B-H24 alloys with dimensions of 100 x 100 x 3mm were joined using FSW machine in Metallurgical and Materials Engineering lab, Suez faculty of Petroleum and Mining Engineering (Egypt) .

All materials provided by CRL METAL CO.LTD (China), First sample, FSW is applied between AA7075-T6 and AZ31B-H24 alloys without interlayer as shown in Fig 1. the second Sample pure Zn foil of 0.2 mm thickness is added between Mg and Al alloys' lapped regions, as shown in Fig 2. The third sample pure Ni foil of 0.1 mm thickness is added between Mg and Al alloys' lapped regions, as shown in Fig 3. The chemical compositions of the base metals and interlayers were conducted using XRF instrument SPECTROMETER Model NITON XL3 T980 GOLD with accuracy 0.5% in the Egyptian Central Metallurgical Research and development Institute, The chemical composition are shown in Tables 1

| Material | Al | Mg | Ni | Zn | Si | Mn | Cu | Fe | Cr | Pb | Cd |
|---|---|---|---|---|---|---|---|---|---|---|---|
| AA7075-T6 | 90 | 2.5 | - | 5.3 | 0.09 | 0.03 | 1.6 | 0.23 | 0.23 | - | - |
| AZ31B-H24 | 2.6 | 96.34 | 0.005 | 0.8 | 0.01 | 0.2 | 0.005 | 0.005 | - | - | - |
| Ni 200 | - | - | 99.7 | - | 0.02 | 0.05 | 0.08 | 0.15 | - | - | - |
| Zn | - | - | - | 99.6 | - | - | 0.002 | 0.04 | - | 0.3 | 0.07 |

Tables 1: Anticipated alloys chemical composition

### 2.2 FSW Process

All the experiments are performed with a tilt angle of 3° with respect to the tool vertical axis and plunge depth of 0.1 mm. the Mg plate is kept at the top and Al at the bottom It is because such a configuration can yield better joint strength by previous empirical experiments implemented inside the metallurgical and materials engineering lab, Suez faculty of Petroleum and Mining Engineering (Egypt), The plate overlapping length is kept at 36 mm. The optimum parameters are taken from previous work implemented by the author on the same material in the first trials to join the members with highest quality.

The optimum parameters of the three samples are given in table 2, table 3 and table 4 respectively.

| **Welding Variables** | | **FSW** |
|---|---|---|
| **Process Type** | | Automatic |
| **Joint Design** | Joint type | Lap |
| | Joint Spacing | Zero |
| | Overlap | 36 mm |
| **Base metals** | 1st Material | AZ31B |
| | 2nd Material | AA 7075 |
| | Thickness | 3 mm |
| | P No. | Not listed |
| **Interlayer** | | Without Interlayer |
| **Gas Shielding** | | Not applicable |
| **Joint restrained** | | fixed anvil |
| **Control method** | | Visual and automatic |
| **Tool Design** | Material | H13 tool steel |
| | Pin Length (mm) | 4.3 |
| | Pin Diameter (mm) | 5.65 |
| | Shoulder Diameter (mm) | 19.95 |
| **Technique** | Welding Speed (V) (mm/min) | 40 |
| | Load ( Kg) | 1250 |
| | Rotation rate (r) (rpm) | 600 |
| | Speed entrance (mm/sec) | 1.5 |
| | Tilt angle | 3° |
| | Fixed Backing | Yes |

Table 2: WPS - without interlayer

| **Welding Variables** | | **FSW** |
|---|---|---|
| **Process Type** | | Automatic |
| **Joint Design** | Joint type | Lap |
| | Joint Spacing | Zero |
| | Overlap | 30 mm |
| **Base metals** | 1st Material | AZ31B |
| | 2nd Material | AA 7075 |
| | Thickness | 3 mm |
| | P No. | Not listed |
| **Interlayer** | | Zn |

| | | |
|---|---|---|
| **Gas Shielding** | | Not applicable |
| **Joint restrained** | | fixed anvil |
| **Control method** | | Visual and automatic |
| **Tool Design** | Material | H13 tool steel |
| | Pin Length (mm) | 4.3 |
| | Pin Diameter (mm) | 5.65 |
| | Shoulder Diameter (mm) | 19.95 |
| **Technique** | Welding Speed (V) (mm/min) | 25 |
| | Load ( Kg) | 480-1000 |
| | Rotation rate (r) (rpm) | 600 |
| | Speed entrance (mm/sec) | 1.5 |
| | Tilt angle | 3° |
| | Fixed Backing | Yes |

Table 3: WPS - with Zn interlayer

| **Welding Variables** | | **FSW** |
|---|---|---|
| **Process Type** | | Automatic |
| **Joint Design** | Joint type | Lap |
| | Joint Spacing | Zero |
| | Overlap | 36 mm |
| **Base metals** | 1st Material | AZ31B |
| | 2nd Material | AA 7075 |
| | Thickness | 3 mm |
| | P No. | Not listed |
| **Interlayer** | | Ni Interlayer |
| **Gas Shielding** | | Not applicable |
| **Joint restrained** | | fixed anvil |
| **Control method** | | Visual and automatic |
| **Tool Design** | Material | H13 tool steel |
| | Pin Length (mm) | 5.05 |
| | Pin Diameter (mm) | 6.15 |
| | Shoulder Diameter (mm) | 19.95 |
| **Technique** | Welding Speed (V) (mm/min) | 35 |
| | Load ( Kg) | 950 |
| | Rotation rate (r) (rpm) | 600 |
| | Speed entrance (mm/sec) | 1.5 |
| | Tilt angle | 3° |
| | Fixed Backing | Yes |

Table 4: WPS - with Ni interlayer

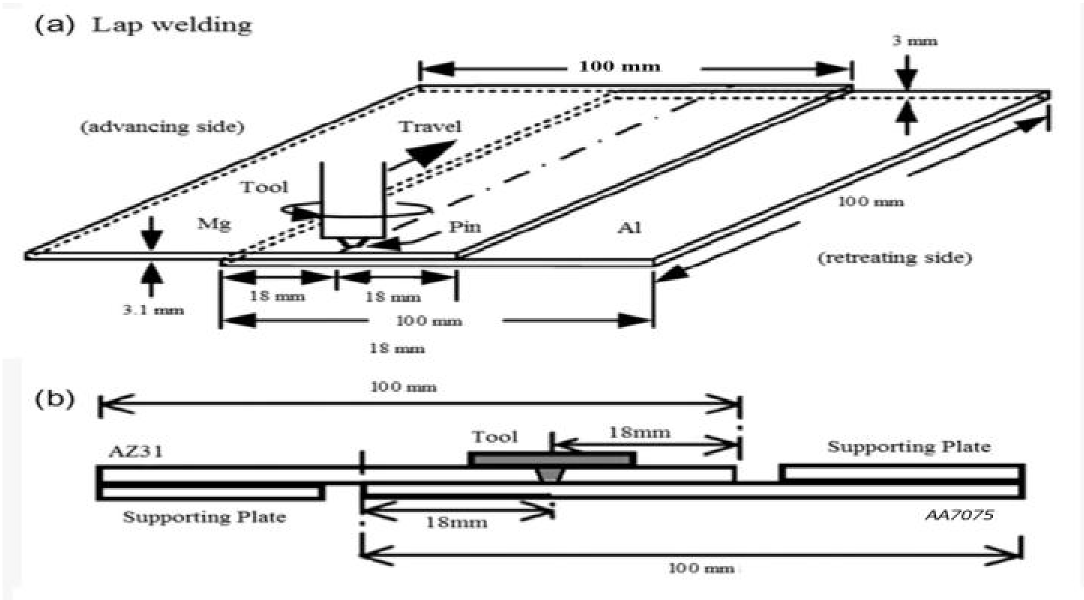


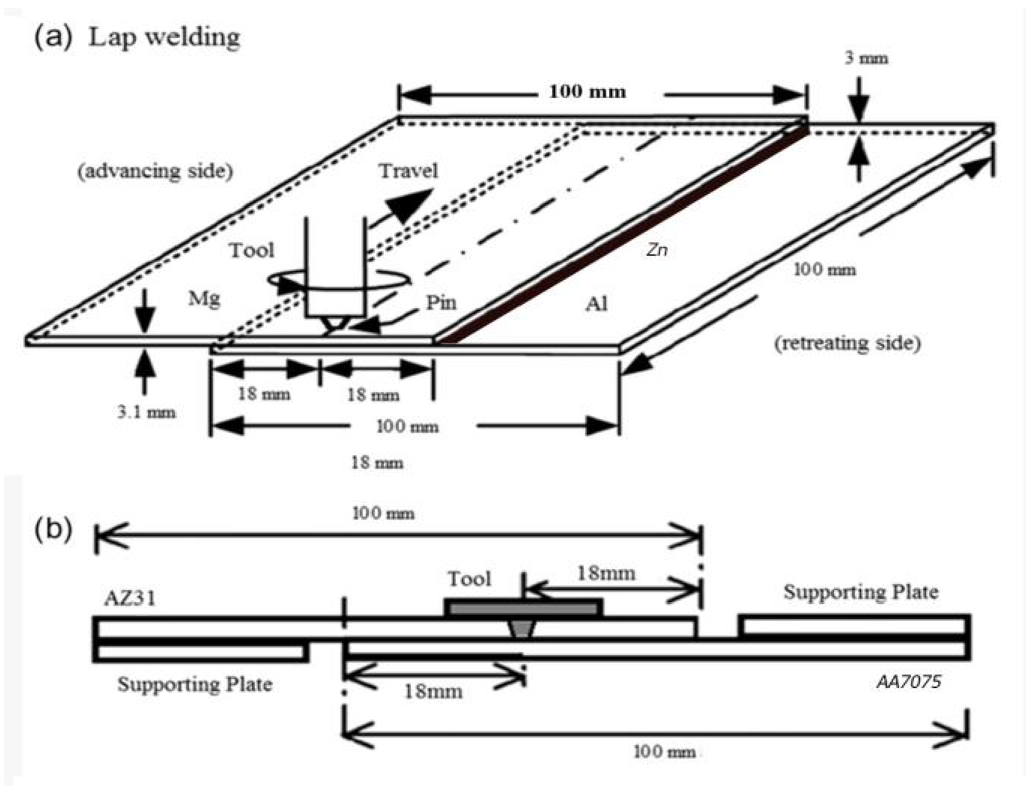


Fig 1 Schematic diagrams of a AA7075 and AZ31B alloys were Lap welded without interlayers.

Figure 2. Schematic diagrams of a AA7075 and AZ31B alloys were Lap welded with Zn interlayers.

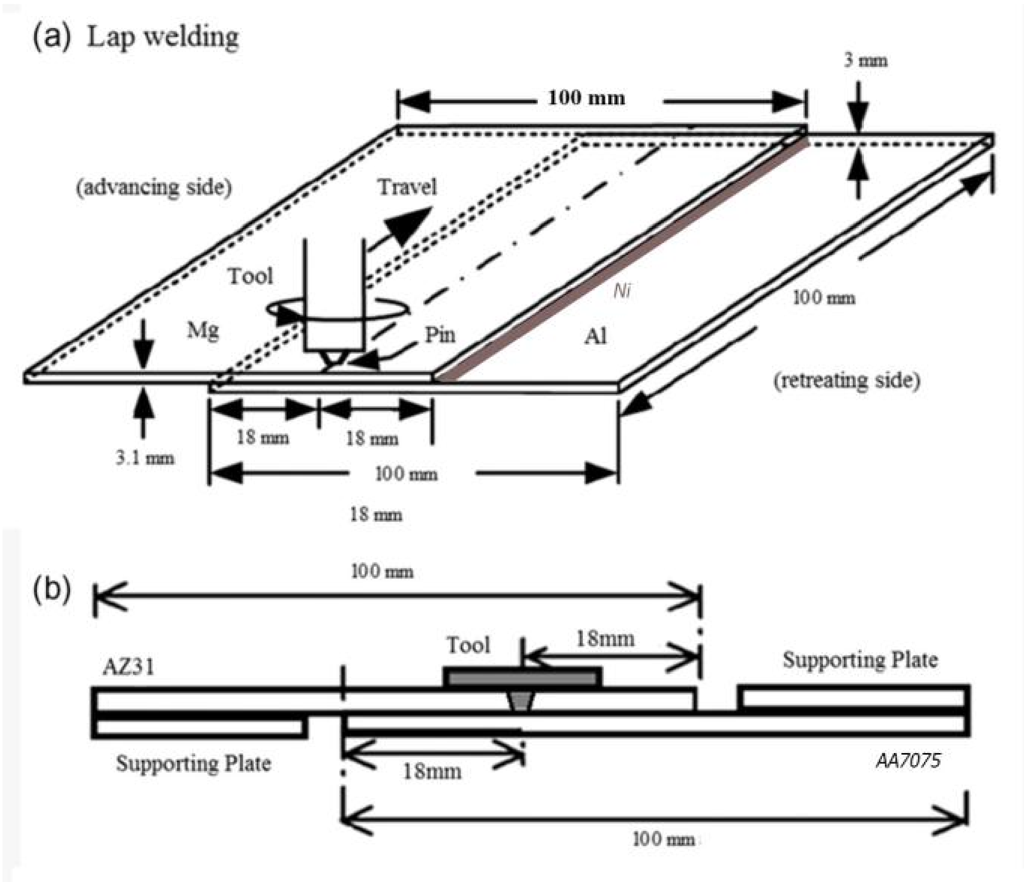


Figure 3. Schematic diagrams of a AA7075 and AZ31B alloys were Lap welded with Ni interlayer.

**2.3 Destructive and Nondestructive Testing**

Visual Testing

| PWPS | without - 1 |
|---|---|
| Interlayer | N.A |
| Coupon | 2 |

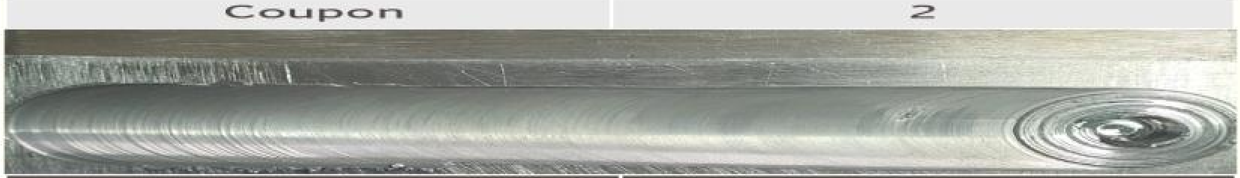

| Variables | FSW |
|---|---|
| Welding Speed (V) (mm/min) | 40 |
| Load ( Kg) | 1250 |

Figure 4 PWPS 01 - Without interlayer

| PWPS | Zn-2 |
|---|---|
| Interlayer | Zn |
| Coupon | 6 |

| Variables | FSW |
|---|---|
| Welding Speed (V) (mm/min) | 25 |
| Load ( Kg) | 750 |

Figure 5 PWPS 02- With Zn interlayer

| PWPS | Ni-3 |
|---|---|
| Interlayer | Ni |
| Coupon | 4 |

| Variables | FSW |
|---|---|
| Welding Speed (V) (mm/min) | 35 |
| Load ( Kg) | 950 |

Figure 6 PWPS 03 –With Ni interlayer

The cross-sectional samples were cut into proper sizes by an electro-discharge machine (cutting locations are illustrated in figure 7 ) and mechanically polished. the specimens were chemical etched by a modified Keller's reagent (150 ml H2O, 2 ml HNO3, 6 ml HCl, 6 ml HF) to unveil the significant features of the Aluminum microstructure.

The same procedure was repeated to investigate the Magnesium side using a solution based on 4.2 g picric acid in mixture of 70 ml ethanol, 10 ml acetic acid and 10 ml distilled water

Quanta FEG 250 Optical microscope and JSM-6610 scanning electron microscope (SEM) equipped with an energy-dispersive X-ray spectroscopy (EDS) facility are used to characterize the microstructure and phase compositions in welds and IMCs be analyzed within the SZ.

Lap shear samples are prepared as per ASTM E8/E8M standard, and tests are done on a computer-controlled universal tensile testing machine at a constant crosshead speed of 1 mm/min at room temperature. two shear samples on each parameter are tested under identical conditions, and their average values are taken for further analysis. The microhardness measurements are conducted on a hardness indentation machine (UHL VMHT 001) at 200 gmf, and 15 s dwell time.

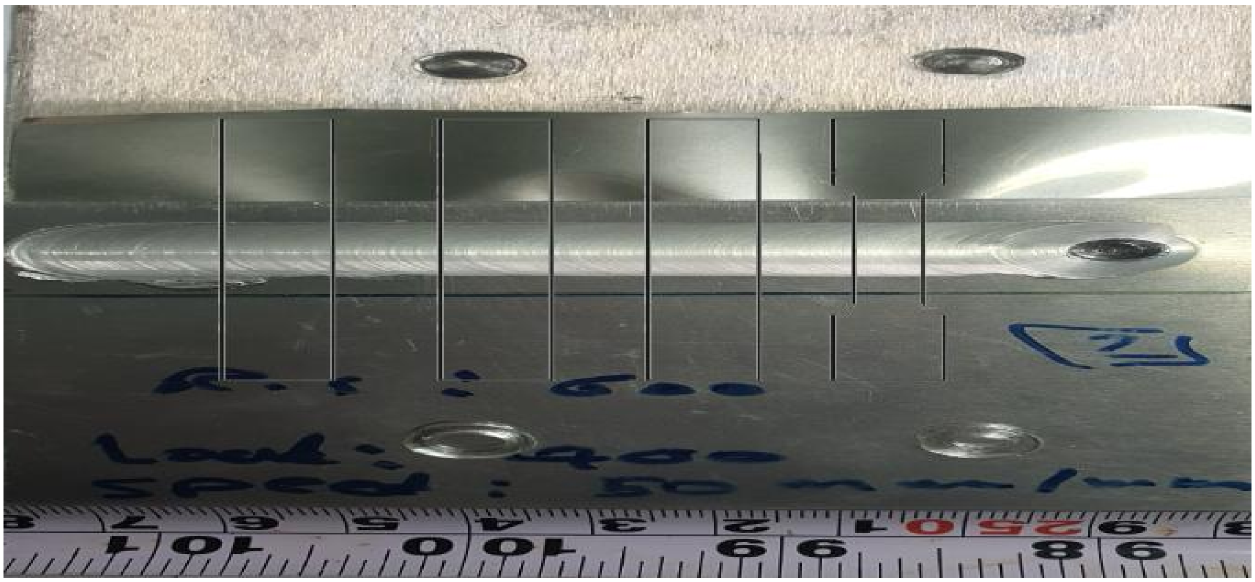

Figure 7: Specimens Cutting Locations

## 3 Results and discussion

### 3.1 Weld Appearances and Macrostructures

FIGs 8. shows the surface appearances of the Al/Mg, Al/Zn/Mg and Al/Ni/Mg joints respectively. In Figure 8a, the surface of the Al/Mg joint is featured by obvious flashes on the weld edges. These flashes are produced in the excreting course of deformed materials from the joint to the surface Al/Zn/Mg and Al/Ni/Mg joints have a relatively smooth surface with flashes, as shown in Figure 8b and Figure 8c.

Homogeneous arc corrugations are observed for all joints, which are formed by the frictional interaction between the rotating tool shoulder and the material surface. Typical keyholes are also generated at the end of the welds as the tool pin retracts from the joint.

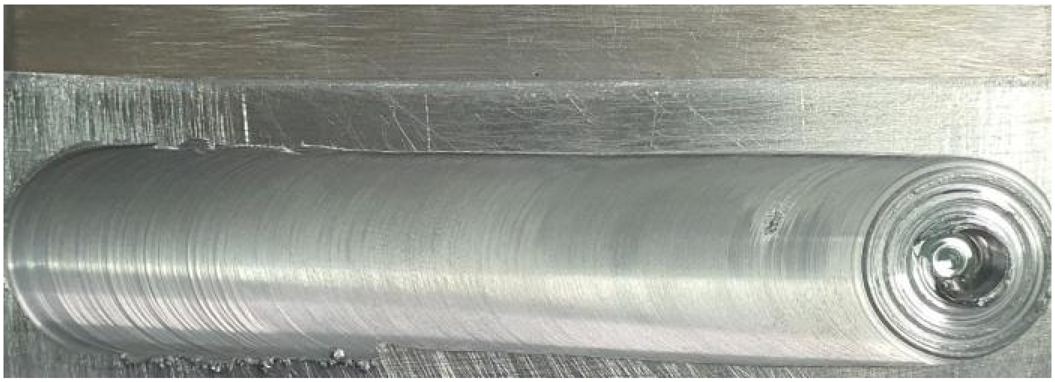

Figure 8a. Schematic diagrams of a AA7075 and AZ31B alloys were Lap welded without interlay

Figure 8b. Schematic diagrams of a AA7075 and AZ31B alloys were Lap welded with Zn interlay

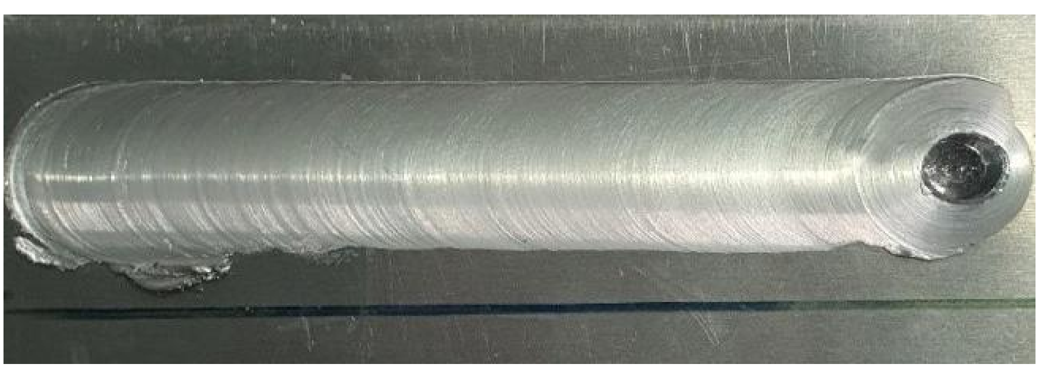

Figure 8c. Schematic diagrams of a AA7075 and AZ31B alloys were Lap welded with Ni interlayer

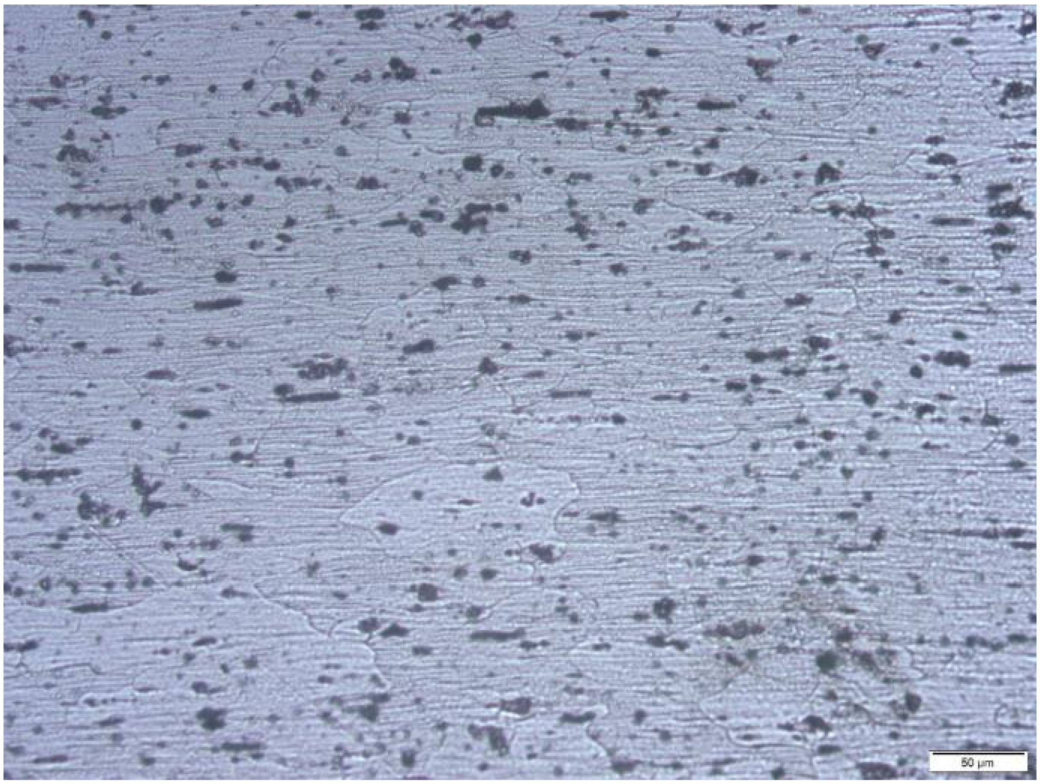


Figure 9. Schematic diagrams Al base metal microstructure

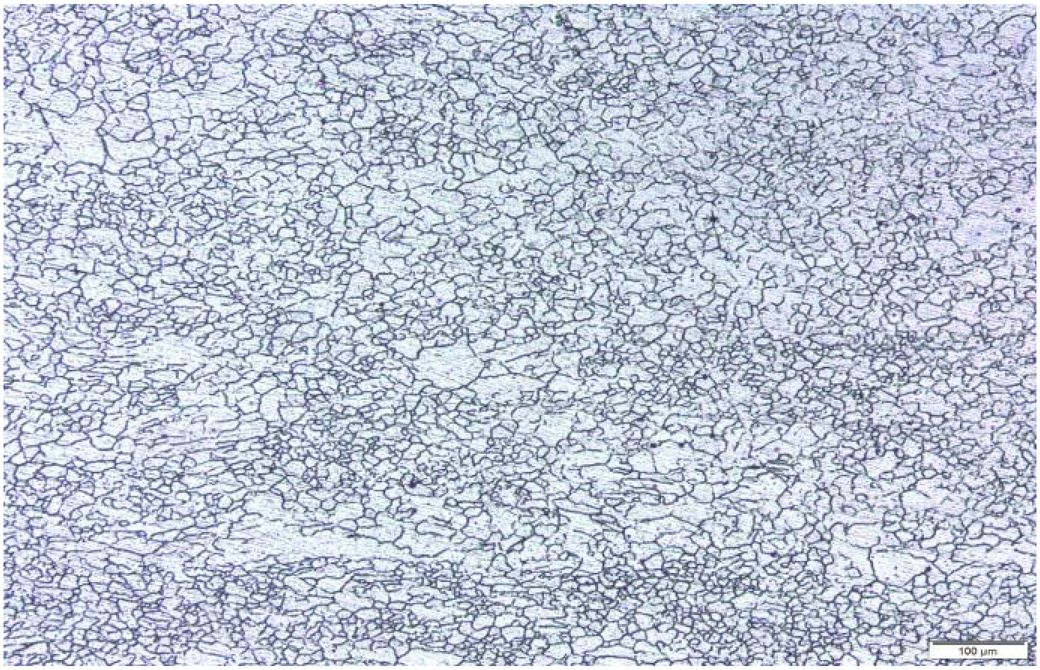


Figure 10. Schematic diagrams Mg Base metal microstructure

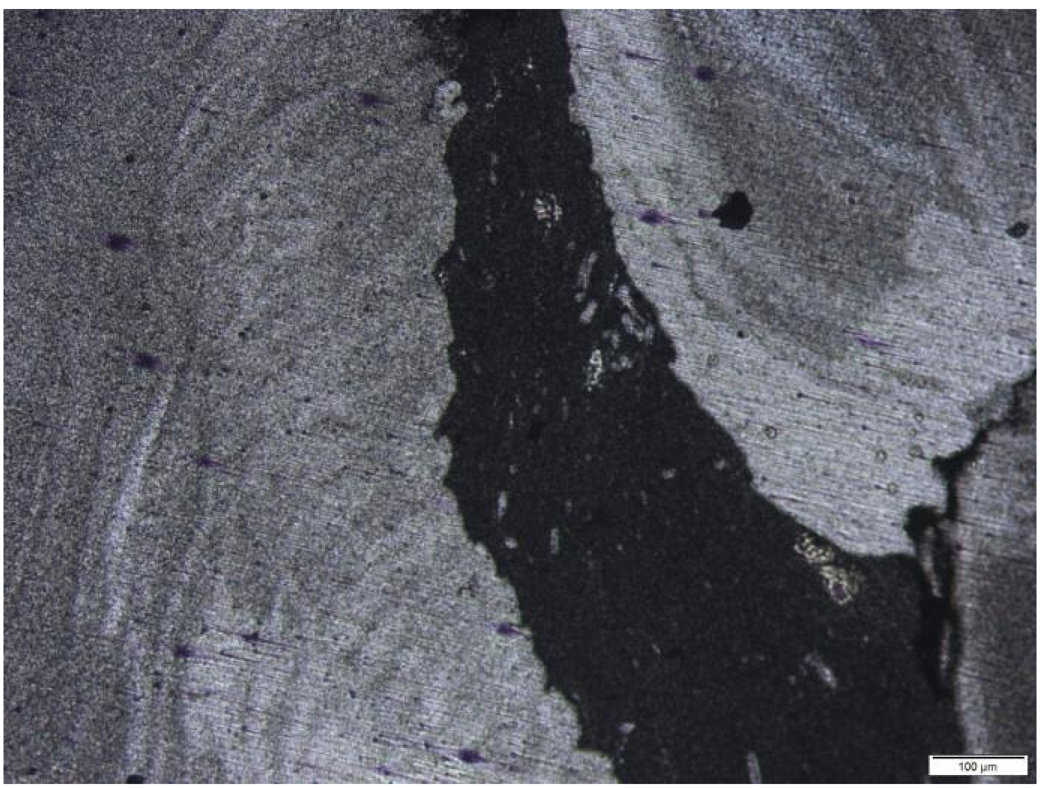

Fig. 11a, optical graphs of the nugget zone of Mg-Al lap joints without interlayer

fig. 11b, optical graphs of the Al side of Mg-Al lap joints without interlayer

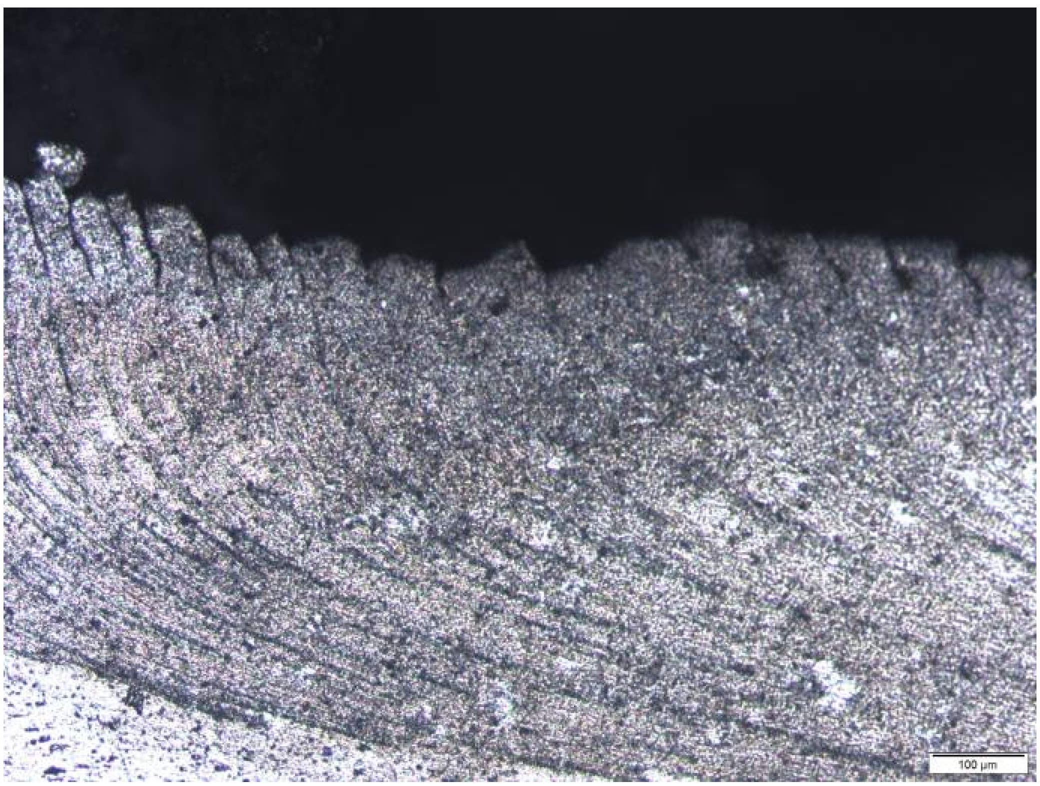


Figure 12 Specimen of AA7075 and AZ31B alloys were welded with Zn Interlayer - Nugget Zone Microstructure

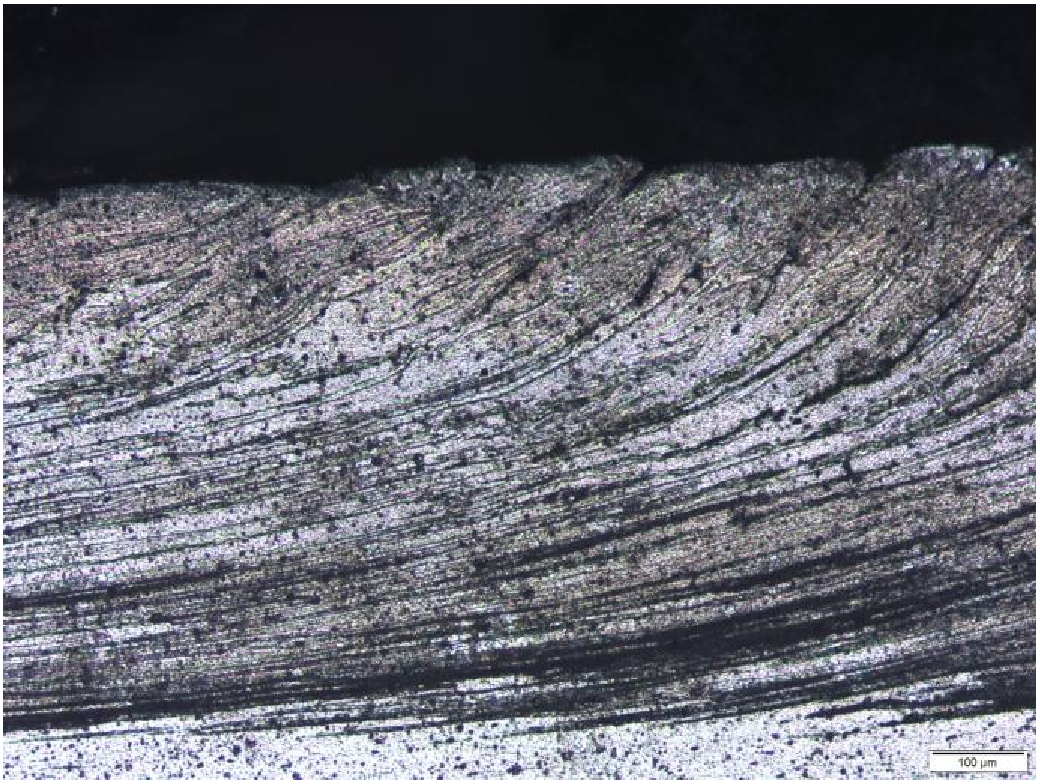


Figure 13 Specimen of AA7075 and AZ31B alloys were welded with Ni Interlayer - Nugget Zone Microstructure

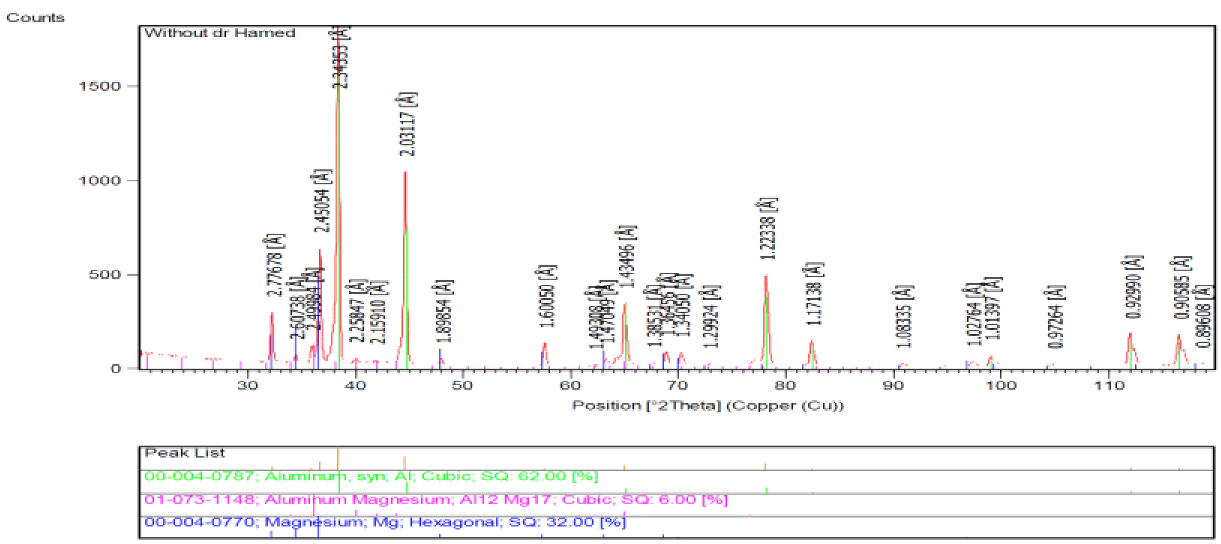


Fig 14, XRD Analysis without interlayer.

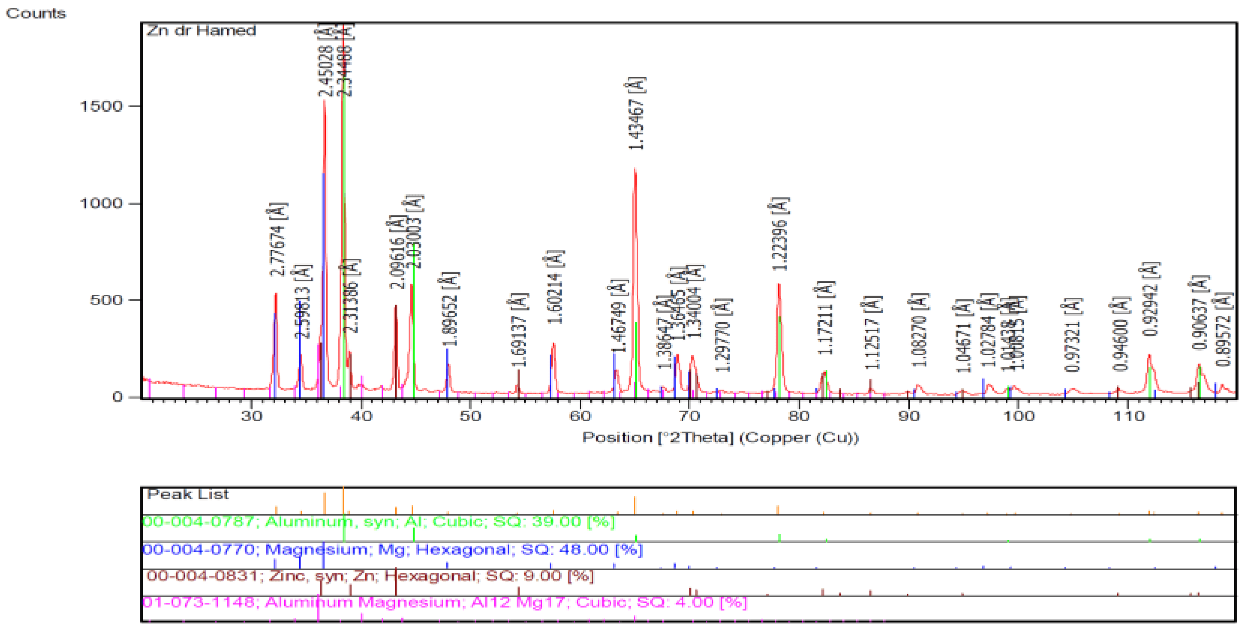


Fig 15, XRD - Zn Interlayer.

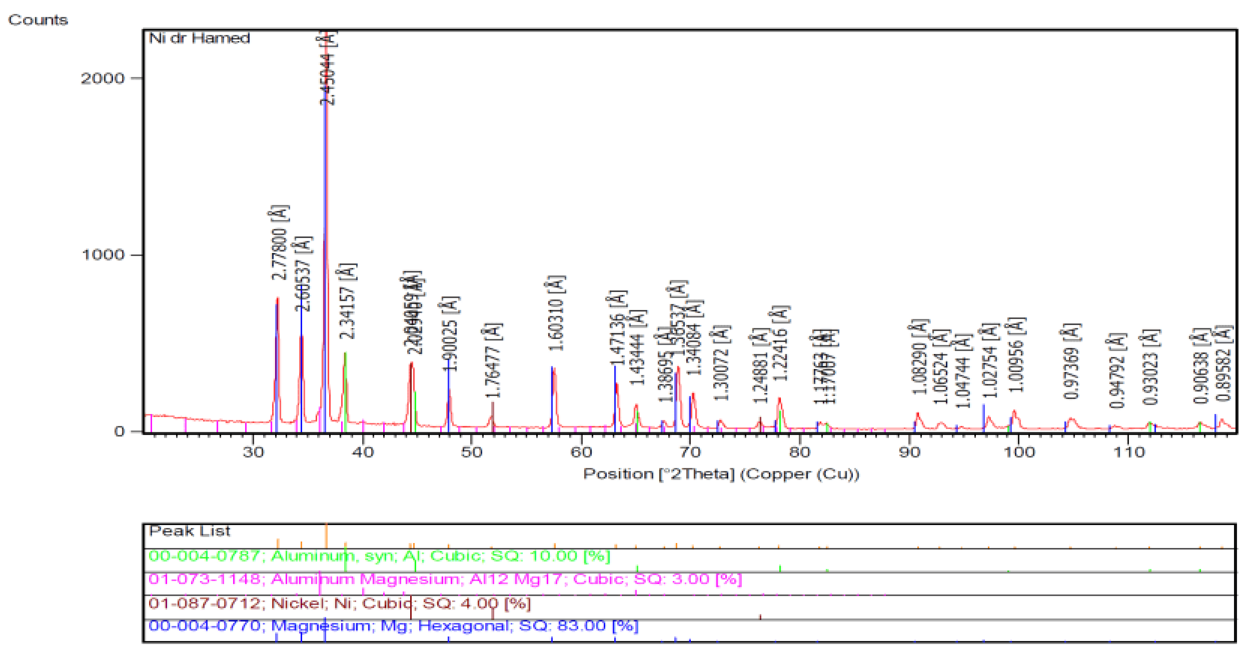


Fig 16, XRD – Ni Interlayer

Fig. 11, optical graphs of the Al side zone of Mg-Al lap joints without interlayer

Fig. 11a shows optical graphs of the nugget zone of Mg-Al lap joints. The weld morphology displays a SZ profile, the accumulation of Al and Mg substrates and their intermixed mixture can be seen at the SZ bottom.

The crack and groove defects are observed at the hook interface for conventional joint without interlayer Fig. 11a. Typically these defects are formed due to inadequate intermixing, higher heat interaction, and IMCs. the hook defect is a common feature of the FSLW process. The hook is formed due to the upward bending of the bottom sheet across the SZ and thermomechanical affected zone (TMAZ) when the tool shoulder exerts downward pressure while plunging into the bottom sheet. The hook's size and orientation enhance the localized stress concentration and favor the crack propagation in the weld region. All together can affect the joint strength severely. With the addition of Ni and Zn interlayers, the weld morphology of the joint is significantly altered.

The Ni and Zn interlayers are substantially thinned in the weld central region while its strips get sheared out and intermix with Al-Mg substrates. The thinning and shearing of the Ni and Zn interlayers in the form of the tiny chips can be due to the rotary action of the tool shoulder and the pin and the frictional resistance offered under shoulder rotation. At the RS, the hook shape is overlapped with the interlayer as a circular section across SZ and TMAZ, while its bottom is extended into the SZ. Across the AS, the hook is stretched towards the Mg plate, separating the TMAZ and SZ regions. The joint made with Ni interlayer does not show any noticeable crack or groove defects (Fig. 8c) while the joint made with zinc interlayer shows small cavities(Fig. 8b) . It infers that both Ni and Zn interlayers might have suppressed these defects via reducing the heat interaction and minimizing the IMCs.

To investigate the effect of Ni and Zn addition on material mixing, the SEM and EDS point scans, specific elemental mapping of the hook regions (for convention and interlayer joints) are made (Figs. 12 and 13). For the conventional joint, the sharp defined Al, Mg interfaces are characterized, attributing inadequate intermixing of both the alloys across their hook contact regions. The EDS scans of points 1 in fig 17 confirm Al as major constitutes, while that of point 3, Mg as the primary element. At these points, the weight percentage (wt.%) of Al and Mg is a deficit to form any IMCs; hence intermetallic formation is impossible. For point 3, the wt.% of Al and Mg show the possibility to form IMCs phase Al3Mg2. it can be inferred that the hook region of the conventional joint may contain Al3Mg2 IMCs phase.

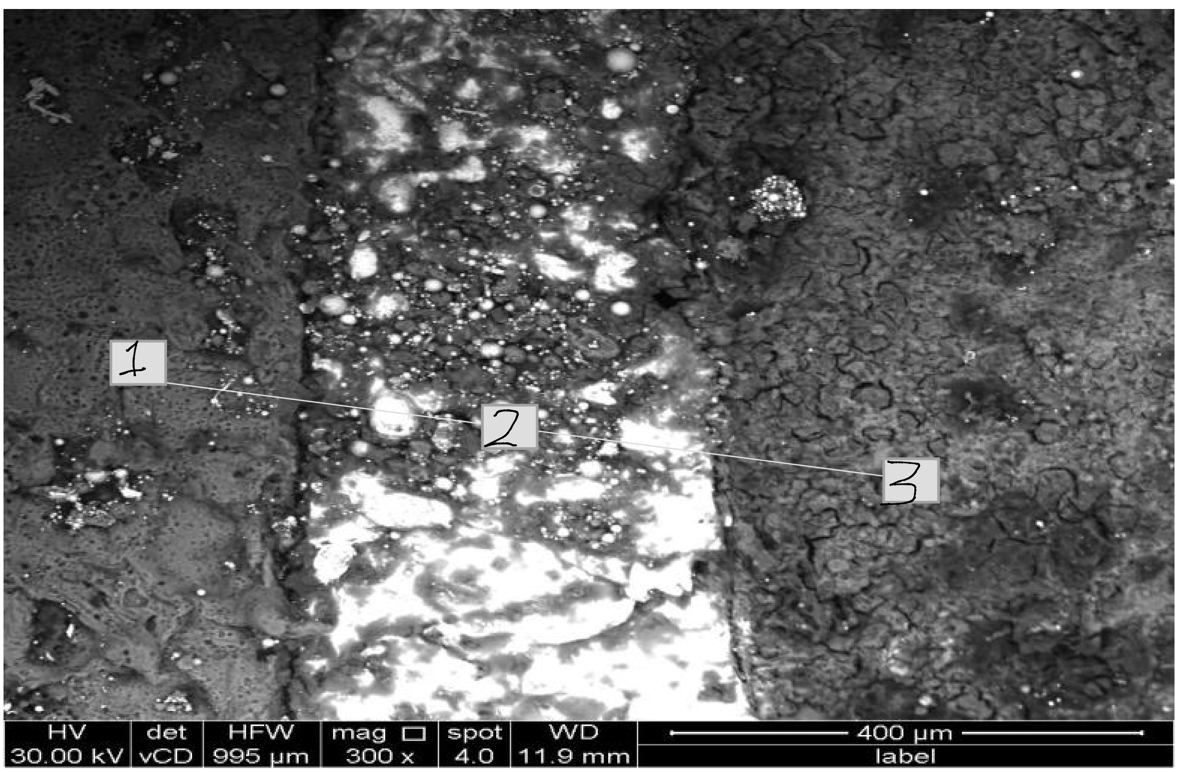


Figure 17: SEM image, lines scans, elemental distribution of the SZ regions without interlayer

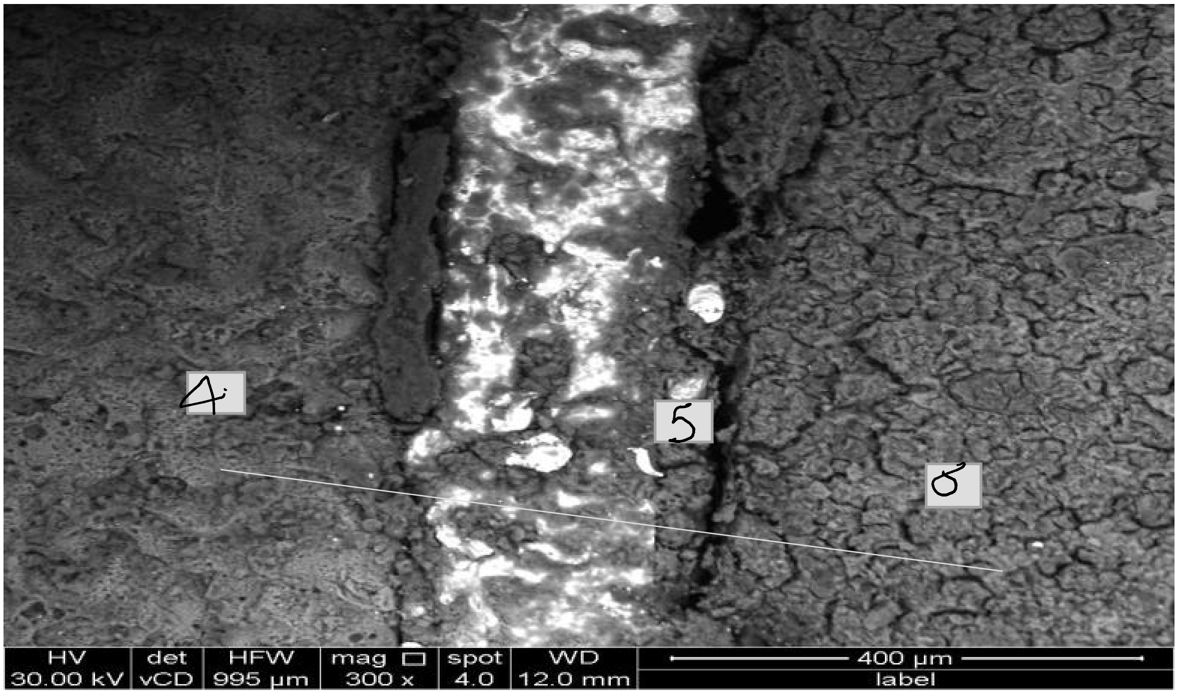


Figure 18: SEM image, lines scans, elemental distribution of the SZ regions with Zn interlayer

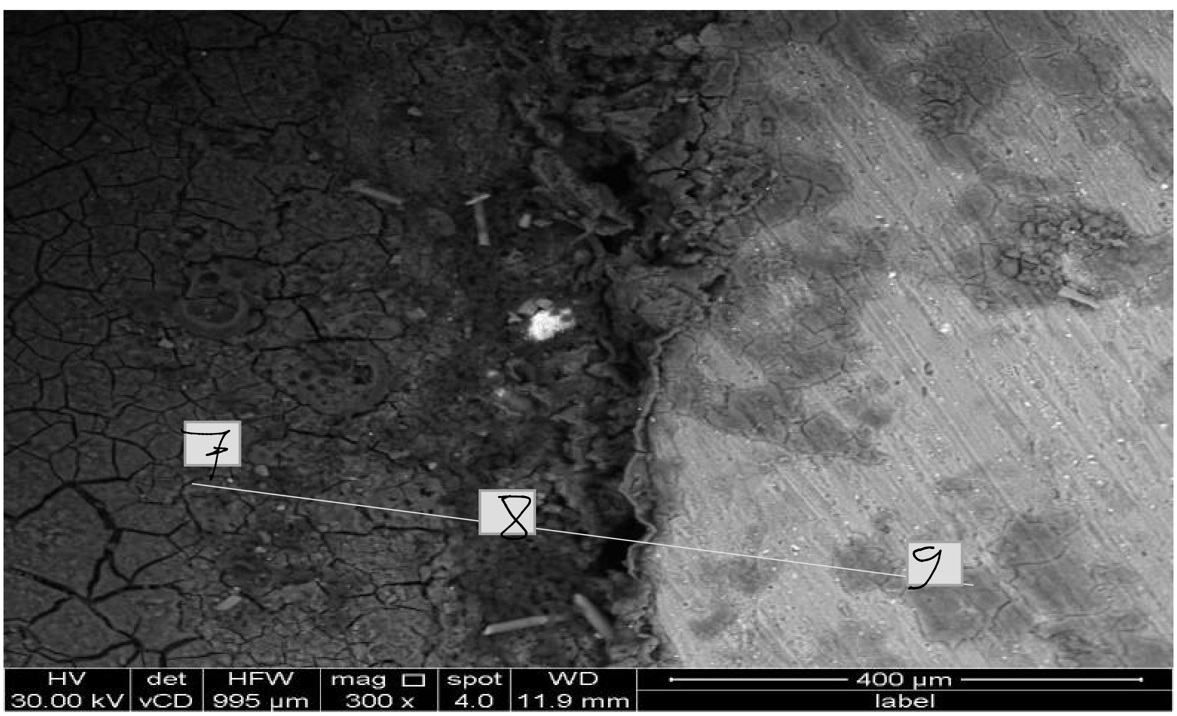

Figure 19: SEM image, lines scans, elemental distribution of the SZ regions with Ni inteFor Ni interlayered joint, the SEM images show the intricate intermixing pattern of Al, Mg, and Ni substrates together across their hook boundaries fig 19. During welding, the melting of the Ni interlayer is not anticipated as the melting point temperature of Ni (1453 °C) is significantly higher than the average maximum temperature reported in the FSW process (450-550 °C). During the FSLW, the sheared interlayer is transformed into the broken tiny flakes in the weld zone. Some of these get intermixed with the Al and Mg substrates, while the rest remain stick at various places with the hook region . As the Ni strips are found to be stick with the Al and Mg substrates, it signifies that some wetting reaction might have occurred between the Mg-Ni and Al-Ni. The intermixing pattern of Ni interlayer can also be understood by elemental mapping As perceived, there is substantial diffusion of Mg and Al alloys with a little penetration of Ni foil. The Ni interlayer participates with Al and Mg substrates to form a complex structure..

The EDS point analysis of the hook region is made to identify the nature of the IMCs formed. As observed, point 8, have major wt.% of Ni compared to Al and Mg fig 19.

Points 7 and 9 cannot form any bi-metallic IMCs phase due to the deficient wt.% of Al and Mg. The wt.% of point 8 show a notable amount of Al, Mg, and Ni, enough to form the IMCs phase.

A close observation of the wt.% of point 8 verifies Al3Ni, Al3Ni2, and Mg2Ni IMCs phases. It shows that the Ni interlayer is efficacious to eliminate the harmful IMCs phase Al3Mg2 via transforming it to Mg-Ni and Al-Ni-based IMCs. Several studies have reported that the Al3Mg2 IMCs phase is chiefly responsible for degrading the joint strength compared to Al12Mg17. The EDS analysis results that point 8 have a major wt.% concentration of Ni while points 7 and 9 have a mixture of Al, Mg, and Ni. It does imply that at RS, there is a higher inter-diffusion of Ni interlayer with Al and Mg substrates compared to AS. The EDS results also show the notable wt.% of Ni element in the hook region, verifying Ni's intermixing with Al and Mg. Thus it is further affirmed that the Ni interlayer can effectively cease the inter-diffusion of Al and Mg substrates and restricts Al-Mg IMCs formation.

For Zn interlayer joint a part of the advancing side of the joint is shown in fig 2 . The Zn poor and rich regions can be observed. Fig 18 shows the Zn rich region at higher magnification. Formation of some thin intermetallic layers is visible in this graph. Fig.18 shows the Mg alloy interface and the banded structure zone on the Mg side. no visible alternating bands or continuous layer of intermetallic can be observed near the Mg interface. The region near Mg interface consists of α (Mg) + Mg-Zn phases, according to the EDS analysis. It can be observed that the regions with unreacted Zn (light regions) increase from the advancing to the retreating side. Considering that the heat input and the exposure time of the material to the high temperature on the retreating side are lower than those in the advancing side, a greater amount of unreacted Zn element will remain on the RD side. The heat input is good enough to make appropriate intermixing of materials and melt a sufficient amount of the Zn interlayer. Moreover, the diffusion of Zn elements to the base materials is easier. Consequently, the formation of Mg-Zn intermetallic compounds prevents the formation of Al-Mg IMCs in the stir zone and interface of the Mg alloy. The presence Zn poor and rich regions (in white color) in the stir zone suggest the non-uniformity of Zn elements in this zone. On the other hand, point 5shows a uniform and homogenous structure without the presence of any Al-Mg IMCs bands near the Mg interface. According to the EDS analysis, the region indicated by points 5 consists of both magnesium and zinc, the amount of magnesium being greater. This suggests that the phase is an α (Mg) + $MgZn_2$

eutectic structure. Mg-Zn eutectic microstructure is famous for its hardness and brittleness. However, the dispersive distribution of Mg-Zn second phase particles can prevent the crack propagation.

The SEM image and EDS line scan of the distribution of main elements (Al, Mg, and Zn) in the Mg and nugget zone interface are shown in Fig. 18. Mg decreased while Zn increased from Mg alloy toward the nugget zone. In addition, the aluminum number increases slightly. The main regions of the nugget close to Mg alloy contain both Mg and Zn elements, as implied by the elemental distribution results. This suggests the presence of uniform eutectic structure in this area. Furthermore, uniform composition is an advantageous property of the joint.

## Conclusions

In this article, we have successfully performed the friction stir lap welding of AA7075-T6 and AZ31B Mg alloys with and without interlayers (Ni and Zn). A comparative analysis is made for the joining processes, and the study is concluded with the following observations.

1. Stronger joints can be produced by adding Ni interlayer across the Mg and Al lapped interface compared to the conventional joint and Zn interlayer joint. The Ni interlayer has ceased the formation of Mg-Al brittle IMCs while favored the formation of Al-Ni and Mg-Ni intermetallic layers across the Al/Ni and Mg/Ni interfaces, respectively.
2. The hook region shows sharply defined edges for the conventional joint. However, these interfaces show complex intermixing of Ni flakes with Al and Mg substrates in Ni interlayer addition. The weld central region showed substrates of Ni, which could be due to the wetting of the Ni interlayer and its shearing during plunging and tool travel.

For the Zn added joints contained Mg and Mg-Zn eutectic structures, Al-Mg-Zn IMC, and solid solutions whereas there were brittle Mg17Al12 and Mg2Al3 IMCs in the Zn-free joints, however

3. In contrast, the Ni interlayer addition has eliminated the formation of Mg-Al intermetallic. Consequently, the fracture occurred across the Mg-Ni interface adjacent to the Mg2Ni IMCs phase for the Ni interlayer joint. The formation of dimple structures suggested a mixed-mode fracture of brittle and ductile across Ni interlayer welds.

4. For Ni interlayered joint, the maximum weld strength reported was 4.39 kN, which was 920 N higher compared to the conventional joint. The maximum micro-hardness in the SZ for the Ni interlayered joint comes out 166.35 HV, which is 70.13 HV lower than its counterpart.

References

1- Eliminating intermetallic compounds via Ni interlayer during friction stir welding of dissimilar Mg/Al alloys Sachin Kumar a,b, Chuansong Wu a,*a MOE Key Lab for Liquid-Solid Structure Evolution and Materials Processing, Institute of Materials Joining, Shandong University, Jinan, 250061, China b Department of Mechanical Engineering, Indian Institute of Science (IISc), Bengaluru, Karnataka, 560012, India. 15 October 2021 2021 The Author(s). Published by Elsevier B.V.

2- Friction Stir Welding of Dissimilar AA7075-T6 to AZ31B-H24 Alloys Published online by Cambridge University Press: 12 December 2017 D. Hernández-García, R. Saldaña-Garcés, F. García-Vázquez, E.J. Gutiérrez-Castañeda, R. Deaquino-Lara and D. Verdera

Musa Bilgin1 · Şener Karabulut1 · Ahmet Özdemir2 - Investigation of Heat-Assisted Dissimilar

3- Friction Stir Welding of AA7075-T6 Aluminum and AZ31B Magnesium Alloys, Published in Procedia Engineering in 2017

4- Microstructure and Corrosion Behaviour of Friction Stir-Welded 6061 Al/AZ31 Mg Joints with a Zr Interlayer, April 2019, Journal of The Electrochemical Society

5- Dissimilar welding of A7075-T651 and AZ31B alloys by gas metal arc plug welding method Published in Procedia Engineering in 2016